ADVANCED FUNCTIONAL MATERIALS
www.afm-journal.de

Humidity-Triggered Self-Healing of Microporous Polyelectrolyte Multilayer Coatings for Hydrophobic Drug Delivery

Xia-Chao Chen, Ke-Feng Ren, Jia-Hui Zhang, Dan-Dan Li, Emily Zhao, Zhong Jonathon Zhao, Zhi-Kang Xu, and Jian Ji**

Layer-by-layer (LbL) self-assemblies have inherent potential as dynamic coatings because of the sensitivity of their building blocks to external stimuli. Here, humidity serves as a feasible trigger to activate the self-healing of a microporous polyethylenimine/poly(acrylic acid) multilayer film. Microporous structures within the polyelectrolyte multilayer (PEM) film are created by acid treatment, followed by freeze-drying to remove water. The self-healing of these micropores can be triggered at 100% relative humidity, under which condition the mobility of the polyelectrolytes is activated. Based on this, a facile and versatile method is suggested for directly integrating hydrophobic drugs into PEM films for surface-mediated drug delivery. The high porosity of microporous film enables the highest loading (≈303.5 μg cm^{-2} for a 15-bilayered film) of triclosan to be a one-shot process via wicking action and subsequent solvent removal, thus dramatically streamlining the processes and reducing complexities compared to the existing LbL strategies. The self-healing of a drug-loaded microporous PEM film significantly reduces the diffusion coefficient of triclosan, which is favorable for the long-term sustained release of the drug. The dynamic properties of this polymeric coating provide great potential for its use as a delivery platform for hydrophobic drugs in a wide variety of biomedical applications.

1. Introduction

Dynamic coatings that can adjust their structures and properties according to environmental stimuli have attracted tremendous interests during recent years.[1–4] Compared to their static counterparts with immutable form and function, such dynamic coatings possess multiple virtues: selected properties of interest can be switched "on" or "off" and conformational or chemical reconfiguration of these coatings endow them with many new functions.[3,5] As a result, various dynamic coatings have been proposed to cope with a wide range of interface-related challenges, including cell behavior manipulation, tunable optics, shape memory, and defect self-healing.[6–11] Layer-by-layer (LbL) self-assemblies, fabricated by alternating deposition of oppositely charged species on the substrates, have inherent potential as dynamic coatings because the interactions between building blocks can easily be modulated by electric field, pH, high salt concentration, light, etc. As a typical example, when LbL films are exposed to low pH, the interchain ionic bonds break and reform after the protonation or deprotonation of polyions, allowing a large scale reorganization of internal structure.[12–17] For instance, poly(allylamine hydrochloride)/poly(acrylic acid) (PAH/PAA) LbL films can cycle between a nanoporous state and a nonporous state by alternating exposure to pH 1.8 and pH 5.5.[15] These thin films with tunable porosity have proven to be ideal for optical technologies such as antireflection coatings.[7]

The LbL technique has also emerged as a striking tool for engineering drug delivery systems (DDSs) with controlled structure and composition.[18–22] In particular, the LbL assemblies can conform to the surfaces of various biomedical devices and serve as host materials enabling controlled delivery of therapeutics.[22] This technique is especially suitable for incorporating the water-soluble charged drugs that have a strong affinity for the components of LbL films.[23–25] However, only a few strategies have been proposed for the incorporation of hydrophobic therapeutics, which makes up about 40% of commercially available drugs.[26] One approach involves the integration of various nanocarriers, such as micelles, cyclodextrins, prodrugs, and liposomes, which can function as vehicles allowing hydrophobic drugs to be incorporated into LbL films.[26–30] Trapping drugs into the hydrophobic nanodomains within LbL films is another option.[31] Although all of these methods have distinctive features and advantages, they may suffer from problems associated with chemical synthesis and complicated operations. In addition, the limited capacity of nanocarriers, nanodomains, and prodrugs makes it difficult to realize high drug loading

X.-C. Chen, Dr. K.-F. Ren, J.-H. Zhang, D.-D. Li, E. Zhao, Dr. Z. J. Zhao, Prof. Z.-K. Xu, Prof. J. Ji
MOE Key Laboratory of Macromolecule Synthesis and Functionalization
Department of Polymer Science and Engineering
Zhejiang University
310027 Hangzhou, P. R. China
E-mail: Renkf@zju.edu.cn; Jijian@zju.edu.cn

DOI: 10.1002/adfm.201503258

unless the number of bilayers is further increased. Therefore, it is desirable to develop a simple and versatile approach to efficiently incorporate hydrophobic drugs into multilayer films fabricated from commercially available building blocks.

More recently, dynamic microporous coatings with alterable porous structures have aroused considerable and widespread interests in a variety of fields, including separation, electronics, drug delivery, and tissue engineering.[32–36] In this work, we developed a dynamic polyelectrolyte multilayer (PEM) coating with self-healing microporous structures (**Scheme 1**). First of all, a nonporous PEM film was assembled from polyethylenimine (PEI) at high pH and PAA at low pH according to the pH-amplified exponential growth mode.[37,38] Microporous structures were created by acid treatment, followed by freeze drying to remove water. The healing of these microporous structures can be triggered at 100% relative humidity (RH), under which condition the mobility of polyelectrolytes is activated. As one potential application of this dynamic platform, we suggest a facile and versatile method of directly integrating a hydrophobic drug (triclosan in this case) into the PEM films for surface-mediated drug delivery (Scheme 1). The high porosity of microporous films enables the highest loading of triclosan to be a one-shot process via wicking action and subsequent solvent removal, thus dramatically streamlining the processes and reducing complexities compared to existing LbL strategies. The self-healing of a drug-loaded microporous PEM film significantly reduces the diffusion coefficient of triclosan, which is favorable for the long-term sustained release of the drug. The dynamic properties of this polymeric coating provide great potential as a delivery platform for hydrophobic drugs in a wide variety of biomedical applications. More importantly, this dynamic strategy could provide a new concept for construction of drug-releasing polymeric coatings since self-healing is a common phenomenon of many polymers.

2. Results and Discussion

2.1. Fabrication of Microporous PEM Films

As the basis of our research, a 15-bilayer PEM film was rapidly fabricated by alternating deposition of PEI at high pH and PAA at low pH according to the pH amplified exponential growth mode.[37,38] After assembly, the PEI/PAA multilayer film was immersed into a bath of acidic solution (pH 2.9) and the formation of porous structures was monitored in situ utilizing optical microscopy. Many microscale pores appeared (**Figure 1**A,B) after exposure to pH 2.9 for 30 min and larger micropores developed when the immersion time was further extended (Figure 1C–E). When exposed to low pH, weak polyions become protonated or deprotonated, and interchain ionic bonds are cleaved and reformed, allowing a large scale reorganization of internal structures.[39] These films were desiccated by freeze drying rather than conventional nitrogen drying before scanning electron microscope (SEM) examination and further applications. This drying method eliminates the capillary pressure gradient in the walls of the pores and prevents the collapses of porous structures during the process of drying.[40] The important advantage of this approach is that the porous structures are well preserved while no chemical cross-linking takes place. The noncrosslinkage of the porous PEM films provides the potential for the mobility of uncrosslinked polyelectrolytes to be activated by certain stimuli and for structural adjustment to occur in comparison with covalently crosslinked films.

Figure 1F–J shows the cross-sectional SEM images of the PEM films that had been exposed to pH 2.9 for different lengths of time. The internal structures of the PEM film with no acid treatment (0 min) appear compact and featureless, while a series of microporous structures could be developed through acid treatment. With an extended treatment time, the thickness of the porous PEM film increased along with enlargement of the pore volume. The film thickness increased by more than 400% after 1 h of acid treatment and by nearly 700% after 2 h. Based on the correspondence between the porous structure and the duration of acid treatment, PEI/PAA multilayer films with desired internal structures can be easily fabricated.

The fraction of the pore volume ($v_{\%}$) within the PEM film was estimated using an equation described in previous studies

$$v_{\%} = \frac{T - T_0}{T} \cdot 100\% \quad (1)$$

in which T_0 and T are the film thickness before and after acid treatment, respectively.[39] The absolute value of pore volume per square centimeter (v_a) of the PEM film was calculated using the formula

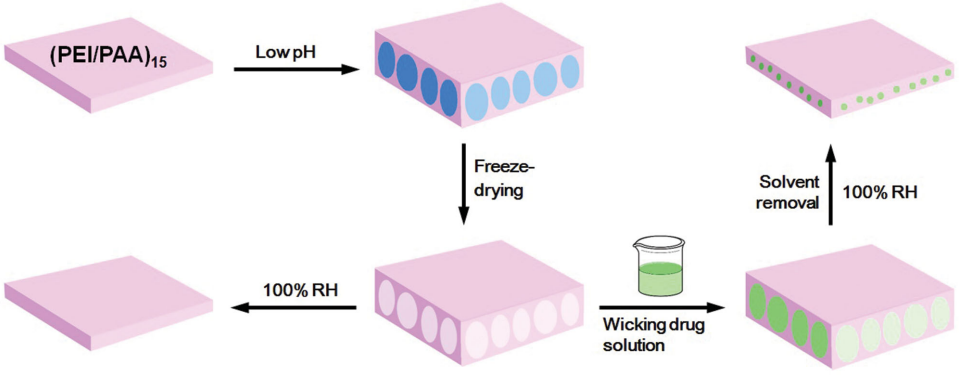

Scheme 1. Fabrication of a dynamic PEM film with self-healing microporous structures and integration of a hydrophobic drug into the film.

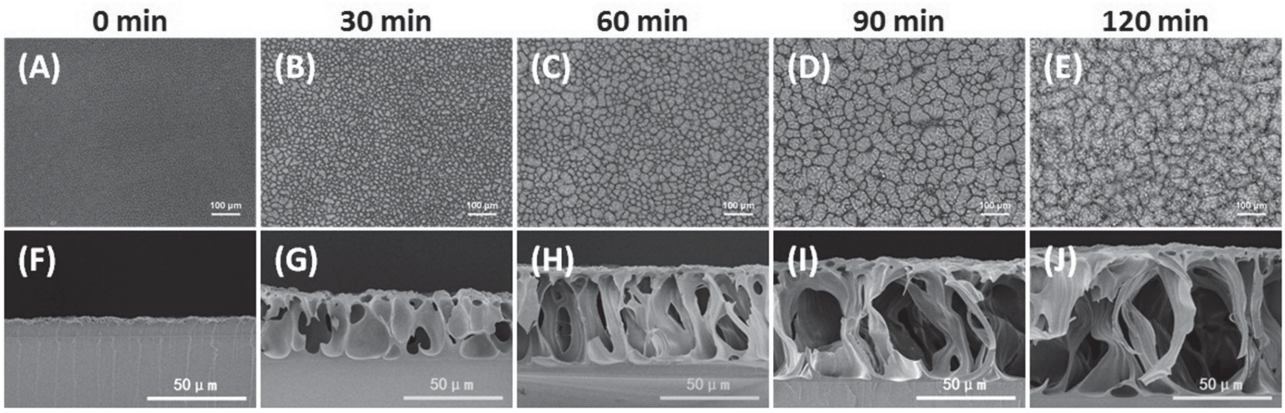

Figure 1. Acid-induced structural evolution of $(PEI/PAA)_{15}$ films over time. Optical microscopy images A–E) and SEM cross-sectional images F–J) of the PEM films after immersion in pH 2.9 solution for 0, 30, 60, 90, and 120 min, respectively. It is important to note that freeze drying was performed to remove water before SEM examination.

$$v_a = 10\ \text{mm} \cdot 10\ \text{mm} \cdot (T - T_0) \quad (2)$$

where both T_0 and T are in millimeters. **Figure 2** shows the dependencies of these calculated results on the duration of acidic treatment. After immersion in the acidic solution for 60 min, the fraction of pore volume climbs to ≈80%, and higher values can be obtained by simply prolonging the immersion time (illustrated by the solid line connecting the square dots in Figure 2). This is sufficient to show that this acid-induced transition is a reliable approach to preparing PEM films with high porosity. As mentioned earlier, the PEI/PAA multilayer film was fabricated by alternating deposition of a weak polycation at high pH and a weak polyanion at low pH on the substrates. The primary advantages of this pH amplified approach are that it can increase the deposited mass per cycle and enhance the growth of polyelectrolyte multilayers effectively.[37] At a constant fraction of pore volume, a larger original thickness of the PEM films implies larger pore volume that can be provided for potential applications. The solid line connecting the circular dots in Figure 2 demonstrates the pore volume per unit area of PEM films as a function of the duration of acidic treatment.

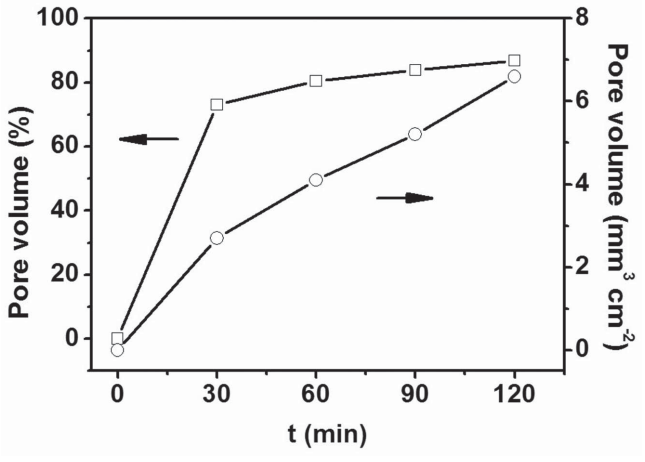

Figure 2. Porosity of PEM films after immersion in the acidic solution (pH 2.9) for various times.

In the case of 60 and 120 min, the pore volumes are ≈4.1 and ≈6.6 $mm^3\ cm^{-2}$, respectively, which are far beyond what have been previously reported for other LbL coatings.[17,39] In this study, the default immersion time at pH 2.9 was set to 60 min for the sake of simplicity.

2.2. Loading of Hydrophobic Drugs

The loading capability of this microporous PEM film was first investigated. **Figure 3**A–F shows the time-lapse images of a microporous PEM film with one end dipped into an ethanol solution of nile red, a brilliant red dye for tracking the liquid level. The liquid front rapidly climbed up the microporous PEM film on the 20 mm × 10 mm glass substrate, and after only 20 s, the film was fully colored. The change in color upward on the film can be attributed to the filling of porous structures through wicking from the dye solution. The occurrence of this phenomenon suggested the presence of numerous connected pores that were well distributed across the whole film. Taking advantage of this kind of interconnected porous network, drugs could be dissolved in solvents (e.g., ethanol, acetone) and loaded into the microporous PEM films by the wicking or absorption method. In our study, ethanol, a common solvent, was used as the dissolving medium and triclosan, a hydrophobic bactericide, was used as the model drug. The advantage of using a volatile solvent lies is that it is able to be quickly removed under vacuum, thus avoiding solvent exchange and eliminating the undesired drug removal.[12] In addition, these processes caused no structural collapse of the microporous PEM films (Figure S1, Supporting Information).

Three different concentrations (20, 60, and 100 mg mL^{-1}) were used to investigate the relationship between drug loading and the concentration of the loading solution. As shown by the solid line in Figure 3G, an approximately linear relationship was found between the former and the latter. The structural stability of the microporous film when immersed in ethanol can be ascribed to the constant absorption capacity of the microporous PEM film during the loading process. In Figure 3G, a dotted line was added to represent the calculated value of the

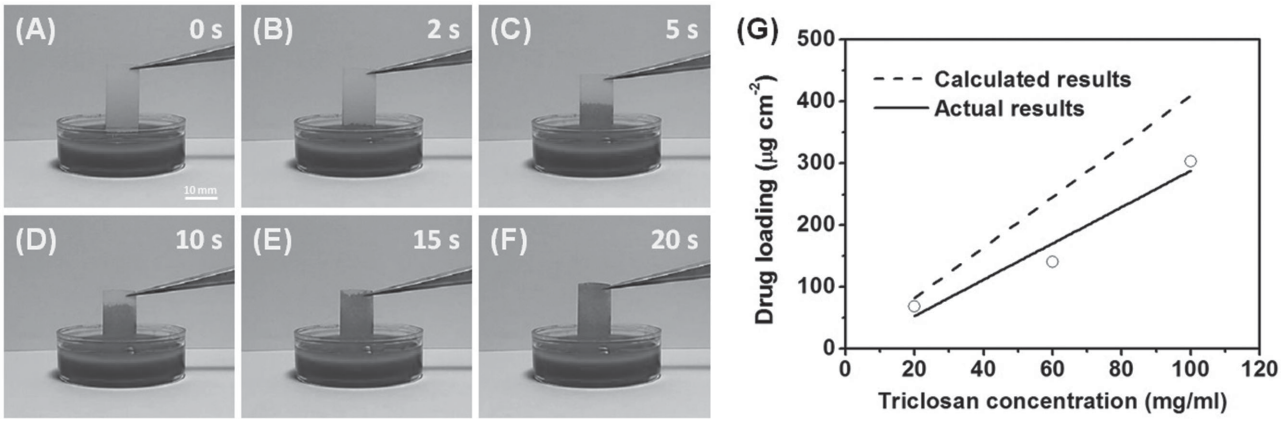

Figure 3. A–F) Nile red, a hydrophobic dye, could be loaded into the microporous PEM film by wicking from its ethanol solution, indicating the presence of abundant open pores across the whole film. G) Plot of actual triclosan loading with respect to the concentration of the triclosan-ethanol solution. A dotted line was added to represent the calculated value of the drug loading as a function of triclosan concentration, assuming that the entire pore volume is available for wicking the drug solution.

drug loading as a function of triclosan concentration, assuming that the entire pore volume is available for wicking drug solution. In the range of concentration studied (20–100 mg mL^{-1}), the calculated values of drug loading were always higher than the actual results, as shown in Figure 3G. This suggests that not all of the pore volume was involved in the wicking of drug solution. The actual ratio (r) of pore volume available for drug loading can be estimated as follows

$$r = \frac{m_a}{m_i} = \frac{m_a}{v \cdot c} \quad (3)$$

where m_a and m_i represent the actual and calculated values of drug loading, respectively, v = 4.1 mm^3 cm^{-2}, and c is the concentration of the triclosan-ethanol solution. By using this formula, r is estimated to be ≈71.3% ± 13.1%. Although a fraction of the pore volume makes no contribution to the drug loading, the loading capacity of the microporous PEM film is still considerable. When the concentration of the loading solution is 20 mg mL^{-1}, the triclosan loading is as high as 4.54 μg cm^{-2} per bilayer (68.1 μg of triclosan per square centimeter in 15 bilayers), which is far beyond what has been previously reported and can be ascribed to the high porosity of the PEM film.[17,39] The high loading of drugs is essential to the long-term maintenance of the local drug concentration above what is called the minimum effective concentration.[41] With increasing drug concentration, the drug loading can be further increased significantly, as shown in **Table 1**. Although the high porosity of microporous films enables the high loading of hydrophobic drug to be a one-shot process, the structural stability of the microporous PEM film when immersed in solvent also makes secondary and tertiary loading possible to further increase the loading amount or even introduce other drugs. The latter might be an effective strategy for constructing a versatile platform for simultaneous delivery of multiple drugs from these surfaces.

Table 1. Drug loading and the concentration of the loading solution have an approximately linear relationship.

Triclosan concentration [mg mL^{-1}]	Drug loading per bilayer [μg cm^{-2}]
20	4.54 ± 1.39
60	9.42 ± 1.25
100	20.23 ± 1.96

2.3. Effect of Humidity on Microporous PEM Films

The drug release behaviors of porous coatings with different structural parameters have been previously reported.[12] It has been shown that an effective way to prolong the release time is to decrease the pore sizes of the coatings. In this sense, the structural adjustment of the microporous PEM films after drug loading assumes great significance. Considering that water has been known as a potent plasticizer for polyelectrolyte complexes, we first studied the effect of humidity on the porous structures of PEM films without drug loading.

The microporous $(PEI/PAA)_{15}$ films were subjected to 75% or 100% RH to investigate the effect of humidity on the porous structures. Because of the correlation between the internal structures and the optical properties,[42] the evolutions of porous PEM films under different humidity conditions was visually observed and monitored by recording the transmittance at 554 nm, as shown in **Figure 4**A–C. The appearance and transmittance of the porous PEM film did not change after it had been exposed to 75% RH for 3 h. However, once exposed to 100% RH, the opaque film became transparent over time and reached a stable transmittance of ≈70% after less than 2 h. The change in transparency could be attributed to the healing of the micropores and subsequent reduction of light scattering between the pore walls and air. To verify this, SEM cross-sectional images of the films exposed to 100% RH for various times were recorded and are shown in Figure 4D. With prolonged exposure to 100% RH, the porous structures collapsed at first and disappeared gradually over the same time-scale as the change in optical properties. In contrast, the internal structures of the porous PEM film stayed the same before and after exposure to 75% RH for 3 h (Figure S2, Supporting Information).

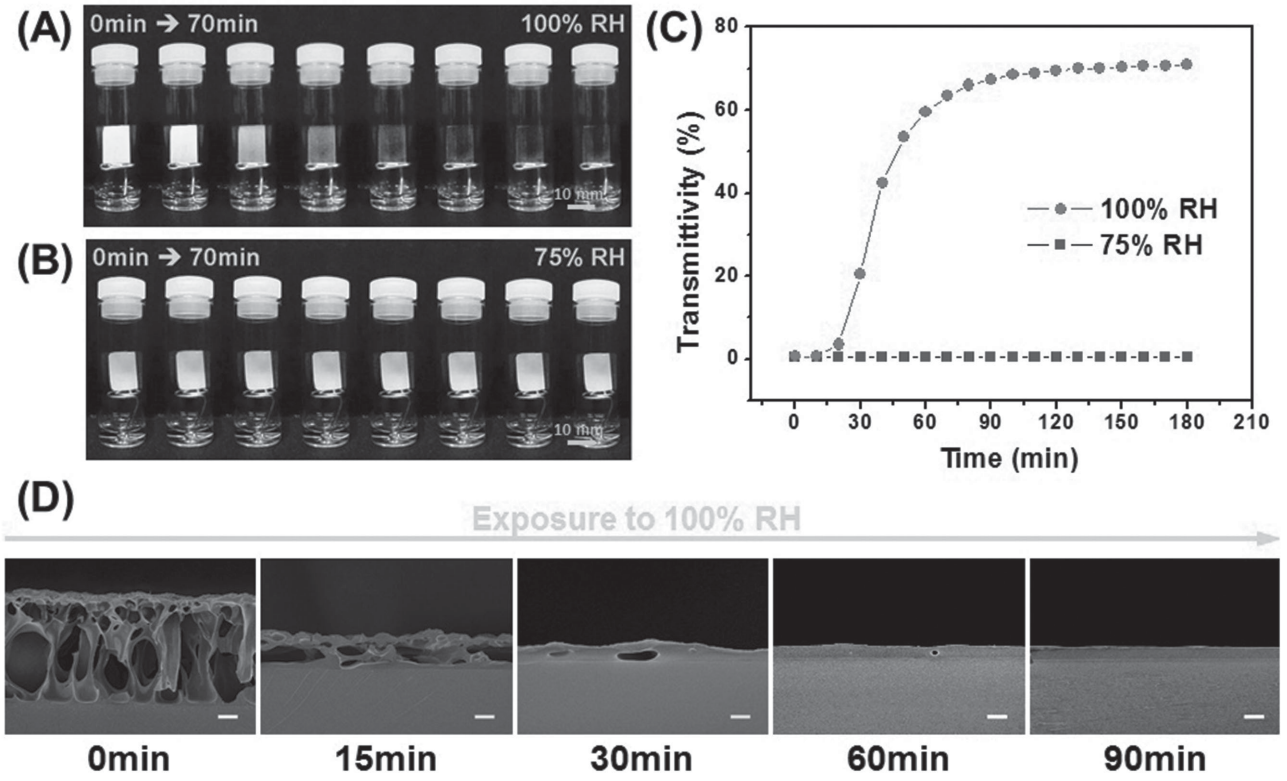

Figure 4. Appearance A,B) andtransmittance C) changes of the porous PEM films exposed to 100% RH and 75% RH, respectively. SEM cross-sectional images D) of the porous PEM film exposed to 100% RH for various times. All of the inset scale bars represent 10 μm.

Both external and internal factors can contribute to this healing process. Previously, many studies have investigated the effects of humidity on the composition and properties of polymeric films.[42–48] One of those general conclusions is that more water can be incorporated into the films with an increase in ambient humidity, and the increase in water content can bring an increase in the free volume available for the movement of chain segments.[42,49,50] For our PEM coatings, the physical characteristics of the PEI/PAA LbL film can provide another key factor for interpreting this dramatic change. Especially important is the charge distribution of polyelectrolytes, which has been investigated primarily to understand the buildup mechanism of PEM films.[51,52] The highly charged polyelectrolytes tend to be kinetically trapped within the films due to their extended polyion size and strong charge binding between ion pairs.[53] In this PEM system, both PEI (p*K*a ≈ 6.5) and PAA (p*K*a ≈ 4.5–5.5) are weak polyelectrolytes with low charge density, and they are assembled into a network that is not tightly cross-linked and therefore is easily disturbed.[37] Besides the free volume, the addition of a solvent of high dielectric constant (e.g., water) can increase the screening of polyion charges within the PEM film and raises the possibility of disrupting electrostatic cross-links, as shown in **Figure 5**. As a result, the effect of water can be to significantly disrupt the crosslinked network and activate the motion of the entire polymer chains, switching the PEI/PAA PEM film from a static state into a fluid state. Sun and co-workers reported a remarkable healing effect on a scratched PEI/PAA PEM film by just exposing it to saturated humidity.[8,54] In that case, the highly softened coating could flow to fill in scratches and recover the integrity of the PEM film. In our case, the healing of porous structures is motivated by the highly mobile polyelectrolytes decreasing the interfacial area and realizing the minimization of the surface energy.

2.4. Healing of the Drug-Loaded Microporous PEM Films

In this work, exposure for 8 h to saturated humidity was performed to heal the microporous PEM films, into which triclosan had been loaded using the method mentioned above,

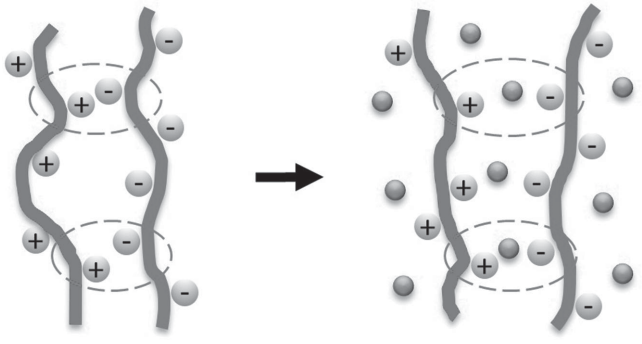

Figure 5. Simplified mechanism of how the water uptake affects the interactions between PEI and PAA. The dark line and the grey line represent PEI and PAA, respectively; the blue dots correspond to the water molecules within the film.

thus eliminating the micropores and integrating the drug into the films (Scheme 1). By adopting such treatment, the original micropores disappeared along with self-aggregation of the drug molecules into microdomains within the PEM films (see Figure S3A–D, Supporting Information). These microdomains are embedded within the PEM films, as confirmed by the SEM cross-sectional data (Figure S3F–H, Supporting Information) and are comprised of triclosan because they can be dissolved away when the thin films are quickly dipped into ethanol (Figure S4, Supporting Information). With the elevation of triclosan concentration, these microdomains increased in quantity and enlarged in volume. The mechanism of the self-aggregation behavior of hydrophobic drugs within the PEM films remains to be further studied.

The effect of the micropore healing on the release profile of triclosan was investigated by measuring the drug release of the PEM films in phosphate buffered saline (PBS) buffer. When immersed into the aqueous medium, the impact of water on the structures of PEM films is not negligible, since liquid water is also able to activate the mobility of polyelectrolytes.[8] Given that, thermal crosslinking was introduced to preserve the structural stability of the film before the release tests by forming amide bonds in the carboxylate-ammonium complexes. Under the same loading condition (60 mg mL^{-1}), the release kinetics of triclosan from the PEM films with and without micropore healing were evaluated. The release profiles of triclosan are plotted in **Figure 6** as the percentage of drug released versus the square root of the release time. The drug release lasted for 130 h in the presence of those original micropores, while micropore healing significantly prolonged the release time to almost 400 h. In Figure 6, the linear relationship between the percentage of triclosan released and the square root of the release time at the early stage indicated that the drug release followed a Fickian diffusion mechanism,[55,56] which can be theoretically described using Higuchi's equation[57]

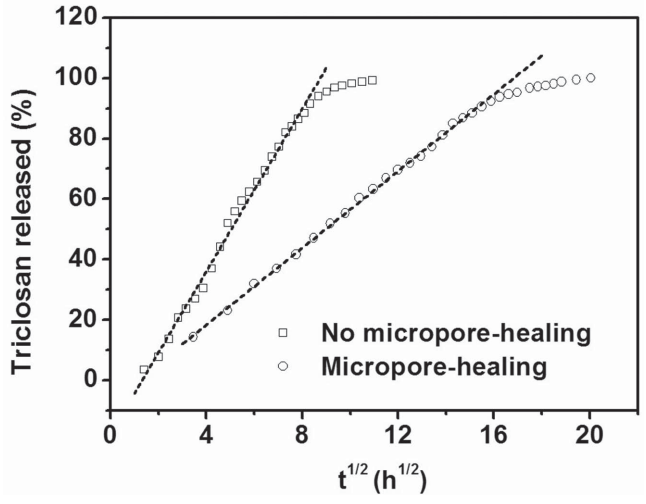

Figure 6. Release profiles of triclosan from the drug-loaded PEM films without A) and with B) micropore healing. The linear relationships between the percentage drug released and the square root of the time of release at the early stage indicated that the drug releases followed a Fickian diffusion mechanism. The closure of those microporous structures is favorable for the sustained release of drugs.

$$f(t) = 4\left(\frac{Dt}{\pi x^2}\right)^{1/2} \quad (4)$$

where $f(t)$ is the percentage of drug released at time t, x is the thickness of the PEM film, $\pi = 3.14$, and D is the diffusion coefficient. The diffusion coefficient can be calculated from the slope of the linear part of the releasing curve using this equation. With the healing of those original micropores, the diffusion coefficient was reduced by two orders of magnitude, from 3.6×10^{-11} to 1.4×10^{-13} cm^2 s^{-1}. Both of these diffusion coefficients are within the usual range for one drug diffusing through a polymer, typically from 10^{-9} to 10^{-19} cm^2 s^{-1}.[55,58,59] Although the drug has been incorporated within the PEM films without micropore healing, the closure of those microporous structures is favorable for sustained release, which can be ascribed to the negative correlation between pore size and release time.[12,60]

2.5. Film Construction onto Metal Stents

The construction of conformal coatings is of great practical significance in the surface modification of medical devices, especially those with complicated shapes.[61,62] In this study, the potential of applying our coatings was assessed by performing an experiment involving the surface of metal stents (**Figure 7**A,B). SEM confirmed the successful construction of microporous PEM films, as

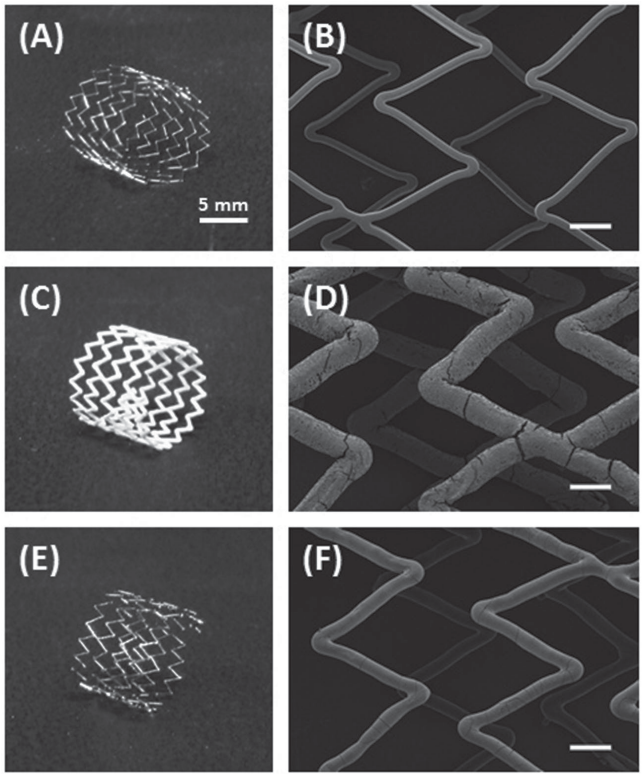

Figure 7. Construction and healing of microporous PEM films on metal stents. A,B) Bare stent. C,D) Stent coated with microporous PEM film. E,F) Stent coated with healed PEM film. (B), (D), and (F) are the SEM images (scale bars are 500 μm) of the stents in (A), (C), and (E), respectively.

shown in Figure 7C,D. Unlike the bare stents that have shiny surface, the coated stents appear white due to the existence of light scattering, which is related to the presence of micropores within the coatings. After exposure to saturated humidity, the appearance of the stents became shiny again (Figure 7E). The SEM image (Figure 7F) shows that the microporous structures were healed along with a thinning of the thickness of the film. Triclosan was loaded into the coating via the approach mentioned above (the concentration of loading solution was set to 60 mg mL^{-1}) and an agar diffusion assay against *Escherichia coli* was performed to test the bactericidal activity of this drug-eluting stent. The drug diffused out of the coating on the stent and formed a clear zone around the sample (see Figure S5, Supporting Information). Since many hydrophobic drugs (e.g., sirolimus, paclitaxel, doxorubicin) can be dissolved in volatile organic solvents that can be removed subsequently under vacuum, our conceptual model could thus be widely applicable.

3. Conclusion

In summary, we demonstrated that humidity can serve as a feasible trigger for activating the self-healing of microporous PEM films, which have great potentials for surface-mediated drug delivery. Microporous structures within PEI/PAA multilayer film can be created by acid treatment and immobilized by freeze drying. The self-healing of these micropores can be triggered by exposure to saturated humidity and the mechanism of this process is related to the activated mobility of polyelectrolytes under this specific condition. Using this dynamic characteristic, a facile and versatile method was developed for integrating hydrophobic drugs into the PEM films for surface-mediated drug delivery. The high porosity of microporous PEI/PAA films enabled the high loading of a hydrophobic drug (triclosan in this case) to be a one-shot process, and the drug loading could be adjusted according to the concentration of the loading solution. After drug loading, exposure to saturated humidity healed those original micropores and triclosan aggregated into many microdomains within the PEM film. The self-healing of a drug-loaded microporous PEM film reduces the diffusion coefficient of triclosan by two orders of magnitude, which is favorable for the long-term sustained release of the drug. The dynamic properties of this polymeric coating provide great potential for its use as a delivery platform for hydrophobic drugs in a wide variety of biomedical applications. We believe that embedding other species such as macromolecules and particles might also be possible utilizing this platform. Also, this dynamic strategy could provide a new concept for construction of drug releasing polymeric coatings since self-healing of a damaged structure is a common phenomenon of many polymers. More importantly, the water-enabled dynamic structural adjustment of the microporous films points to their great potentials in the fabrication of adjustable biological scaffolds, variable capacitors, and other dynamic materials.

4. Experimental Section

Materials: PAA (M_w = 100 000) and poly(ethyleneimine) (PEI, branched, M_w = 25 000) were purchased from Sigma-Aidrich. Triclosan was obtained from Aladdin. PBS was obtained from Sangon Biotech (Shanghai, China). The deionized (DI) water (>18 MΩ cm) used in all experiments was filtered through a Millipore Milli-Q water purification system. The pH values of PEI and PAA aqueous solutions were adjusted utilizing 0.1 M HCl or 0.1 M NaOH. The pH 2.9 water was prepared by adjusting the pH of Milli-Q water using 0.1 M HCl. All materials were used as received.

Construction of Microporous PEM Films: Glass substrates were immersed in freshly prepared piranha solution (30% H_2O_2/98% H_2SO_4 = 3/7 V/V) for 40 min and then rinsed with Milli-Q water thoroughly. PEM films were constructed by alternately immersing the precleaned substrates into PEI solution (1 mg mL^{-1}, pH 9.0) for 15 min and PAA solution (3 mg mL^{-1}, pH 2.9) for 15 min. Between each deposition step, the substrates were rinsed with Milli-Q water and blown dry by nitrogen. This process was repeated until PEM films with the desired number of bilayers were obtained. In this paper, PEM film will be referred to as $(PEI/PAA)_n$, where n is the number of bilayers. The formation of microporous structures was achieved by dipping the as-prepared PEM films into pH 2.9 water for a predetermined time. After that, the films were freeze-dried to remove the water and retain the porous structures. Scanning electron microscopy (SEM, Hitachi S4800, Japan) was performed to monitor the morphologic changes within the PEM films.

Healing of Microporous PEM Films: When the condensation and evaporation of water are at equilibrium in a small, sealed container, a salt solution at a definite concentration and at a constant temperature has a fixed partial vapor pressure of water and hence defines a fixed relative humidity.[8,63] Thus, equilibrium water vapors over saturated NaCl solution and purified water at room temperature were employed to, respectively, establish 75% RH and 100% RH environment. Once exposed to either 75% RH or 100% RH, the appearance and transmittance of the porous PEM films were recorded periodically using a digital camera (Cyber-shot DSC H50, Sony) and an UV–vis spectrophotometer (UV-2550, Shimadzu, Japan).

Loading and Release of Triclosan: The microporous PEM films were dipped partially into a solution of triclosan in ethanol (60 mg mL^{-1}) for 1 min to fill the pores with drug solution through wicking action. The films were taken out and put into a vacuum chamber to remove the ethanol. To measure the actual loading, triclosan can be extracted by ethanol from the microporous PEM films and analyzed using a UV–vis spectrophotometer. After solvent removal, the films were exposed to 100% RH for 8 h to eliminate the micropores and embed the drug in the films. The distribution state of triclosan within the PEM film was investigated utilizing optical microscopy and SEM. The triclosan-loaded PEM films were immersed into PBS (pH 7.4, 37 °C) to investigate the release kinetic. The PBS was frequently replaced with a fresh solution at appropriate time points to ensure constant release conditions and that the released drug concentrations were in the linear range of the calibration curve of absorbance at 263 nm versus concentration. The solutions were analyzed using the UV–vis spectrophotometer.

Zone Inhibition Test: Zone inhibition testing was carried out using *E. coli* (ATCC 8739). The drug-loaded metal stent was placed onto a nutrient agar plate that had been seeded with 0.2 mL bacterial suspension (1.0×10^7 CFU mL^{-1}, in PBS buffer). The plate was examined for a zone of inhibition after incubation at 37 °C overnight.

Supporting Information

Supporting Information is available from the Wiley Online Library or from the author.

Acknowledgements

This research was supported by Zhejiang Provincial Natural Science Foundation of China under Grant No. LR15E030002, the Key Science Technology Innovation Team of Zhejiang Province (Grant No. 2013TD02),

the National Natural Science Foundation of China (51333005, 21374095), the National Basic Research Program of China (2011CB606203), Research Fund for the Doctoral Program of Higher Education of China (20120101130013), International Science and Technology Cooperation Program of China (2014DFG52320), and State Key Laboratory of Molecular Engineering of Polymers (Fudan University) (K2015-10).

Received: August 4, 2015
Revised: September 27, 2015
Published online: November 5, 2015

[1] J. S. Mohammed, W. L. Murphy, *Adv. Mater.* **2009**, *21*, 2361.
[2] E. V. Skorb, H. Mohwald, *Adv. Mater.* **2013**, *25*, 5029.
[3] J. A. Burdick, W. L. Murphy, *Nat. Commun.* **2012**, *3*, 1269.
[4] J.-B. Fan, C. Huang, L. Jiang, S. Wang, *J. Mater. Chem. B* **2013**, *1*, 2222.
[5] R. Klajn, *Chem. Soc. Rev.* **2014**, *43*, 148.
[6] J. Wang, J. Li, N. Li, X. Guo, L. He, X. Cao, W. Zhang, R. He, Z. Qian, Y. Cao, Y. Chen, *Chem. Mater.* **2015**, *27*, 2439.
[7] J. Han, Y. Dou, M. Wei, D. G. Evans, X. Duan, *Angew. Chem. Int. Ed.* **2010**, *49*, 2171.
[8] X. Wang, F. Liu, X. Zheng, J. Sun, *Angew. Chem. Int. Ed.* **2011**, *50*, 11378.
[9] J. Gensel, T. Borke, N. P. Perez, A. Fery, D. V. Andreeva, E. Betthausen, A. H. Muller, H. Mohwald, E. V. Skorb, *Adv. Mater.* **2012**, *24*, 985.
[10] B. Su, S. Wang, Y. Wu, X. Chen, Y. Song, L. Jiang, *Adv. Mater.* **2012**, *24*, 2780.
[11] J. Wang, L. Lin, Q. Cheng, L. Jiang, *Angew. Chem. Int. Ed.* **2012**, *51*, 4676.
[12] M. C. Berg, L. Zhai, R. E. Cohen, M. F. Rubner, *Biomacromolecules* **2006**, *7*, 357.
[13] G. M. Lowman, P. T. Hammond, *Small* **2005**, *1*, 1070.
[14] X. Huang, J. D. Chrisman, N. S. Zacharia, *ACS Macro Lett.* **2013**, *2*, 826.
[15] J. Hiller, J. D. Mendelsohn, M. F. Rubner, *Nat. Mater.* **2002**, *1*, 59.
[16] J. Hiller, M. F. Rubner, *Macromolecules* **2003**, *36*, 4078.
[17] J. L. Lutkenhaus, K. McEnnis, P. T. Hammond, *Macromolecules* **2008**, *41*, 6047.
[18] X. T. Zheng, L. Yu, P. Li, H. Dong, Y. Wang, Y. Liu, C. M. Li, *Adv. Drug Delivery Rev.* **2013**, *65*, 1556.
[19] W. Yuan, Z. Lu, H. Wang, C. M. Li, *Adv. Funct. Mater.* **2012**, *22*, 1932.
[20] S. Pavlukhina, S. Sukhishvili, *Adv. Drug Delivery Rev.* **2011**, *63*, 822.
[21] D. Cui, J. Jing, T. Boudou, I. Pignot-Paintrand, S. De Koker, B. G. De Geest, C. Picart, R. Auzely-Velty, *Adv. Mater.* **2011**, *23*, H200.
[22] A. N. Zelikin, *ACS Nano* **2010**, *4*, 2494.
[23] X. Wang, L. Zhang, L. Wang, J. Sun, J. Shen, *Langmuir* **2010**, *26*, 8187.
[24] U. Manna, M. J. Kratochvil, D. M. Lynn, *Adv. Mater.* **2013**, *25*, 6405.
[25] C. Wu, S. Aslan, A. Gand, J. S. Wolenski, E. Pauthe, P. R. Van Tassel, *Adv. Funct. Mater.* **2013**, *23*, 66.
[26] B. S. Kim, S. W. Park, P. T. Hammond, *ACS Nano* **2008**, *2*, 386.
[27] P. M. Nguyen, N. S. Zacharia, E. Verploegen, P. T. Hammond, *Chem. Mater.* **2007**, *19*, 5524.
[28] Y. X. Sun, K. F. Ren, Y. X. Zhao, X. S. Liu, G. X. Chang, J. Ji, *Langmuir* **2013**, *29*, 11163.
[29] M. Michel, Y. Arntz, G. Fleith, J. Toquant, Y. Haikel, J.-C. Voegel, P. Schaaf, V. Ball, *Langmuir* **2006**, *22*, 2358.
[30] N. Thierry, P. Kujawa, C. Tkaczyk, F. O. M. Winnik, L. Bilodeau, M. Tabrizian, *J. Am. Chem. Soc.* **2005**, *127*, 1626.
[31] T. Boudou, P. Kharkar, J. Jing, R. Guillot, I. Pignot-Paintrand, R. Auzely-Velty, C. Picart, *J. Controlled Release* **2012**, *159*, 403.
[32] L. Xue, J. Zhang, Y. Han, *Prog. Polym. Sci.* **2012**, *37*, 564.
[33] I. Tokarev, S. Minko, *Adv. Mater.* **2009**, *21*, 241.
[34] I. Tokarev, S. Minko, *Adv. Mater.* **2010**, *22*, 3446.
[35] J. Huang, J. M. Mazzara, S. P. Schwendeman, M. D. Thouless, *J. Controlled Release* **2015**, *206*, 20.
[36] S. E. Reinhold, K. G. Desai, L. Zhang, K. F. Olsen, S. P. Schwendeman, *Angew. Chem. Int. Ed.* **2012**, *51*, 10800.
[37] J. Fu, J. Ji, L. Shen, A. Kuller, A. Rosenhahn, J. Shen, M. Grunze, *Langmuir* **2009**, *25*, 672.
[38] J. Ji, J. Fu, J. Shen, *Adv. Mater.* **2006**, *18*, 1441.
[39] J. D. Mendelsohn, C. J. Barrett, V. V. Chan, A. J. Pal, A. M. Mayes, M. F. Rubner, *Langmuir* **2000**, *16*, 5017.
[40] C. A. García-González, M. C. Camino-Rey, M. Alnaief, C. Zetzl, I. Smirnova, *J. Supercrit. Fluids* **2012**, *66*, 297.
[41] K. Park, *J. Controlled Release* **2014**, *190*, 3.
[42] H. H. Hariri, A. M. Lehaf, J. B. Schlenoff, *Macromolecules* **2012**, *45*, 9364.
[43] A. Vidyasagar, C. Sung, R. Gamble, J. L. Lutkenhaus, *ACS Nano* **2012**, *6*, 6174.
[44] S. W. Lee, D. Lee, *Macromolecules* **2013**, *46*, 2793.
[45] K. Trenkenschuh, J. Erath, V. Kuznetsov, J. Gensel, F. Boulmedais, P. Schaaf, G. Papastavrou, A. Fery, *Macromolecules* **2011**, *44*, 8954.
[46] A. J. Nolte, M. F. Rubner, R. E. Cohen, *Macromolecules* **2005**, *38*, 5367.
[47] R. Kohler, I. Donch, P. Ott, A. Laschewsky, A. Fery, R. Krastev, *Langmuir* **2009**, *25*, 11576.
[48] K. E. Secrist, A. J. Nolte, *Macromolecules* **2011**, *44*, 2859.
[49] P. Blasi, S. S. D'Souza, F. Selmin, P. P. DeLuca, *J. Controlled Release* **2005**, *108*, 1.
[50] R. M. Hodge, T. J. Bastow, G. H. Edward, G. P. Simon, A. J. Hill, *Macromolecules* **1995**, *29*, 8137.
[51] C. Picart, J. Mutterer, L. Richert, Y. Luo, G. D. Prestwich, P. Schaaf, J. C. Voegel, P. Lavalle, *Proc. Natl. Acad. Sci. USA* **2002**, *99*, 12531.
[52] P. J. Yoo, N. S. Zacharia, J. Doh, K. T. Nam, A. M. Belcher, P. T. Hammond, *ACS Nano* **2008**, *3*, 561.
[53] Y. H. Kim, Y. M. Lee, J. Park, M. J. Ko, J. H. Park, W. Jung, P. J. Yoo, *Langmuir* **2010**, *26*, 17756.
[54] Y. Li, S. Chen, M. Wu, J. Sun, *Adv. Mater.* **2012**, *24*, 4578.
[55] S. P. Lyu, R. Sparer, C. Hobot, K. Dang, *J. Controlled Release* **2005**, *102*, 679.
[56] P. L. Soo, L. Luo, D. Maysinger, A. Eisenberg, *Langmuir* **2002**, *18*, 9996.
[57] T. Higuchi, *J. Pharm. Sci.* **1961**, *50*, 874.
[58] J. Siepmann, F. Lecomte, R. Bodmeier, *J. Controlled Release* **1999**, *60*, 379.
[59] C. G. Pitt, R. Jeffcoat, R. A. Zweidinger, A. Schindler, *J. Biomed. Mater. Res.* **1979**, *13*, 497.
[60] N. Dan, *Colloids Surf., B* **2015**, *126*, 80.
[61] H. Chang, K. F. Ren, J. L. Wang, H. Zhang, B. L. Wang, S. M. Zheng, Y. Y. Zhou, J. Ji, *Biomaterials* **2013**, *34*, 3345.
[62] J. L. Wang, B. C. Li, Z. J. Li, K. F. Ren, L. J. Jin, S. M. Zhang, H. Chang, Y. X. Sun, J. Ji, *Biomaterials* **2014**, *35*, 7679.
[63] R. Kugler, J. Schmitt, W. Knoll, *Macromol. Chem. Phys.* **2002**, *203*, 413.